Tribology International 42 (2009) 213–219

Contents lists available at ScienceDirect

Tribology International

journal homepage: www.elsevier.com/locate/triboint

An advanced Park's vectors approach for bearing fault detection

Jafar Zarei *, Javad Poshtan

Department of Electrical Engineering, Iran University of Science and Technology, Narmak 1684413114, Tehran, Iran

ARTICLE INFO

Article history:
Received 24 November 2007
Received in revised form
1 June 2008
Accepted 4 June 2008
Available online 31 July 2008

Keywords:
Fault detection
Induction motor
Bearing
Park's vector

ABSTRACT

Induction motors vibrations, caused by bearing defects, result in the modulation of the stator current. In this research, a method based on Park's vector approach for bearing fault detection using three-phase stator current analysis is presented. In order to evaluate the ability of the proposed method several experiments are performed, and sets of data are gathered before and after using defective bearings. Both localized and distributed defects are evaluated using this method. The experimental results from our study suggest that the proposed method provides a powerful and general approach to incipient fault detection.

1. Introduction

Induction motors are critical components of many industrial processes and are frequently integrated in commercially available equipments. Safety, reliability, efficiency, and performance are some of the major concerns of induction motor applications [1]. Although induction motors are reliable, they are subjected to some failures. Therefore, in the past two decades, there has been substantial amount of research to provide new condition monitoring techniques for induction motors mostly based on analyzing vibration signals, or other signals such as current, and hence a number of commercial tools are available in this area [1–7]. In some factories, a very expensive scheduled maintenance is performed in order to prevent sudden motor failures. Therefore, there is a considerable demand to reduce maintenance costs and prevent unscheduled downtimes for electrical drive systems, especially for induction motors [3]. The results of recent studies show that bearing problems account for 40% of all machine failures [5]. Therefore, this type of fault must be detected as soon as possible to avoid fatal breakdowns of machines that may lead to loss of production. Bearing defects may be categorized as "distributed" or "local" [8]. The dominant mode of failure in rolling element bearings is local, including the spalling of races or rolling elements. Localized defects generate a series of impact vibrations every time a running roller passes over the surface of a defect. The amplitude and period of this signal are related to the position of defect, speed and bearing dimensions. Therefore, vibration analysis is a conventional method for bearing fault detection [2–4]. Although vibration analysis has been used for mechanical fault detection for many decades, since the vibration produced by defect is also modulated on the stator current, and this signal can be easily measured for condition monitoring and control purposes, more recent studies on induction motors concentrate on monitoring of electrical signals such as stator current [1–6]. Motor current signature analysis (MCSA) provides a noninvasive approach to obtain information about bearing health using already available line current.

Dependence between characteristic defect frequency in vibration signal and that of current signal was addressed first in 1994 by analyzing the spectrum of vibration and current signals [5]. FFT is the simplest frequency domain analysis method. Because the impact vibration generated by a bearing defect has relatively low energy, it is often overwhelmed by noise with higher energy and vibration generated from other macro-structural components. Therefore, it is difficult to identify the bearing defect in the spectra using conventional FFT methods. As a result, Fourier analysis makes it difficult to recognize faulty condition from the normal operating condition of the motor.

In order to overcome FFT problems and improve signal-to-noise ratio, advanced signal processing methods have been used recently.

In 1997, an adaptive statistical time–frequency method was used for the detection of bearing defects by stator current analysis [9]. The key idea in the method is to transform motor current into a time–frequency spectrum to capture the time variation of the frequency components and to analyze the spectrum statistically to distinguish faulty conditions from the normal operating conditions of the motor. This method was used for broken rotor bar and

* Corresponding author. Tel.: +98 21 772 40492; fax: +98 21 772 40490.
E-mail addresses: jzarei@iust.ac.ir (J. Zarei), jposhtan@iust.ac.ir (J. Poshtan).

0301-679X/$ - see front matter © 2008 Elsevier Ltd. All rights reserved.
doi:10.1016/j.triboint.2008.06.002

bearing fault detection in 1999 [10]. Since the method is based on a training approach, a comprehensive database is needed. Therefore, the method has a drawback in cases where a comprehensive database is not accessible.

In recent years, more advanced signal processing methods such as wavelet analysis and wavelet packet analysis have been used [11–13]. These methods require more computational effort and are not very successful in detecting defect location using MCSA. In order to overcome these problems, the idea of using Park's vector to precisely locate a fault and, at the same time, to reduce the computational complexity was proposed by the authors in Refs. [17–19]. An almost similar idea was presented in Ref. [20]. In their work, however, the case when the characteristic defect frequency is above the power line frequency is not properly considered. It should be noted that in practice it is not always possible to detect a fault without considering all frequency components modulated in the current signal. This has been verified in one of the experimental results in our work. In this paper, considering the fact that the characteristic defect frequency may be greater or less than the power line frequency, we have developed the relations and performed simulations for each case separately.

2. Characteristic defect frequency

Local defects or wear defects cause periodic impulses in vibration signals. Amplitude and period of these impulses are determined by shaft rotational speed, fault location, and bearing dimensions. The frequencies of these impulses considering different defect locations as in Fig. 1 are obtained by Eqs. (1)–(4) [8].

Fundamental cage frequency is given by

$$f_c = \frac{f_s}{2}\left(1 - \frac{d}{D}\cos(\alpha)\right) \tag{1}$$

Ball defect frequency is two times the ball spin frequency and can be calculated as

$$f_{bd} = \frac{D}{d} f_s \left(1 - \frac{d^2}{D^2}\cos^2(\alpha)\right) \tag{2}$$

Inner race defect frequency is given by

$$f_{id} = n(f_s - f_c) = \frac{n f_s}{2}\left(1 - \frac{d}{D}\cos(\alpha)\right) \tag{3}$$

Outer race defect frequency is given by

$$f_{od} = n f_c = \frac{n f_s}{2d}\left(1 - \frac{d}{D}\cos(\alpha)\right) \tag{4}$$

In Eqs. (1)–(4) f_s is the shaft rotation frequency, n the number of rollers, d the roller diameter, D the pitch diameter of the bearing, and α is the contact angle as shown in Fig. 1.

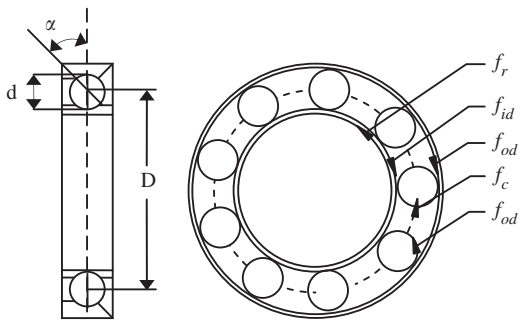

Fig. 1. Bearing dimension and characteristic defect frequencies.

It should be noted that from Eq. (4) specific information concerning the bearing construction is required to calculate the exact characteristic frequencies. However, these characteristic race frequencies can be approximated for most bearings with 6–12 balls by

$$f_{id} = 0.6 \times n \times f_s, \quad f_{od} = 0.4 \times n \times f_s \tag{5}$$

Since the mechanical vibrations produce anomalies in the air gap flux density, they result in the modulation of stator current. These frequencies can be calculated by [5]

$$f_{bng} = |f_e \pm m \times f_v| \tag{6}$$

where $m = 1, 2, 3, \ldots$, f_e is the electrical power supply frequency, and f_v the one of the characteristic vibration frequencies which are calculated by Eqs. (1)–(4). Therefore a defect generates components in both vibration and current signals. As the impact vibration generated by a bearing fault has relatively low energy, it is often overwhelmed by noise with higher energy and vibration generated from other macro-structural components. Therefore, it is difficult to identify the bearing fault in the spectra using the conventional FFT method, and hence advanced signal processing techniques are needed.

In this study, advanced Park's vector approach is proposed for induction motor bearing fault detection. Park transformation is the transformation of three-phase electrical machine parameters to a two-phase machine, using the d and q axes. It is shown that related components to fault in Park's vector modulus spectrum are multiplied by $3i_f$. This advantage provides easier incipient fault detection.

3. Park's vector approach

In a balanced three-phase induction motor, the sum of stator currents is zero. Therefore, only two currents are sufficient for processing and the third one can be obtained from the other two phases [14]. A suitable representation is the use of Park's vector as a function of main phase variables (i_a, i_b, i_c), giving the current Park's vector components (i_d, i_q) as

$$i_d = \sqrt{\frac{2}{3}} i_a - \frac{1}{\sqrt{6}} i_b - \frac{1}{\sqrt{6}} i_c, \quad i_q = \frac{1}{\sqrt{2}} i_b - \frac{1}{\sqrt{2}} i_c \tag{7}$$

In an ideal condition, when only fundamental harmonics exist (with no unwanted harmonics such as odd harmonics in stator current due to asymmetry in motor structure and/or power supply), i_d and i_q Eq. (7) have physical meanings, and are simplified in steady state as

$$i_d = \frac{\sqrt{6}}{2} I_m \sin(\omega t), \quad i_q = \frac{\sqrt{6}}{2} I_m \sin\left(\omega t - \frac{\pi}{2}\right) \tag{8}$$

where I_m is the supply phase maximum current value (amperes), ω the angular supply frequency (radians per second) and, finally, t is the time (seconds). Given these conditions, the current's Park vector modulus is constant.

Under ideal conditions, for a healthy motor, Lissajou's curve $i_q = f(i_d)$ has a circular shape, centered at the origin and having a diameter equal to the stator current corresponding to the state of operating of the motor. In the case of faulty motor, the Lissajou's curve changes in shape and in thickness because of the harmonics presence generated by the fault. The first strategy of this method is to compare both curves of Lissajou's in both cases of the motor that is with and without fault during its operating. This approach has been used for broken rotor bar detection [14–16].

Under abnormal conditions, such as the bearing damage, Eq. (8) is no longer valid. However, without loss of information we can still work with i_d and i_q in Eq. (7). It has been shown that i_d–i_q pattern differs from each other in healthy machine and under open phase or stator-unbalance faults. Different i_d–i_q patterns have been

shown for faults in rectifier diodes and power switches for ac drive systems and for broken rotor bars in ac induction motors [14].

The use of Park's transformation by itself is not good enough for fault diagnosis for a number of reasons. First, it is not obvious if patterns are unique for different faults. Besides, classification is very difficult if noise and practical problems are considered. However, as mentioned above, the transformation keeps all information in the currents while reduces the number of variables from three to two. In order to solve this problem, Park's vector modulus spectrum is proposed.

4. Fault detection using Park's vector approach

Under ideal conditions, stator currents can be expressed as

$$\begin{aligned} i_a(t) &= i_f \cos(2\pi f_e t - \alpha_0) \\ i_b(t) &= i_f \cos\left(2\pi f_e t - \frac{2\pi}{3} - \alpha_0\right) \\ i_c(t) &= i_f \cos\left(2\pi f_e t + \frac{2\pi}{3} - \alpha_0\right) \end{aligned} \tag{9}$$

where i_f and α_0 are fundamental supply phase current, and initial phase angle of fundamental phase current, respectively.

Considering first and secondary harmonics only, the three-phase stator currents can be expressed as

$$\begin{aligned} i_a(t) &= i_f \cos(2\pi f_e t - \alpha_0) + i_{dl} \cos[2\pi(f_e - f_v)t - \beta_l] \\ &\quad + i_{dr} \cos[2\pi(f_e + f_v)t - \beta_r] \\ i_b(t) &= i_f \cos\left(2\pi f_e t - \alpha_0 - \frac{2\pi}{3}\right) + i_{dl} \cos\left[2\pi(f_e - f_v)t - \beta_l - \frac{2\pi}{3}\right] \\ &\quad + i_{dr} \cos\left[2\pi(f_e + f_v)t - \beta_r - \frac{2\pi}{3}\right] \end{aligned}$$

$$\begin{aligned} i_c(t) &= i_f \cos\left(2\pi f_e t - \alpha_0 + \frac{2\pi}{3}\right) + i_{dl} \cos\left[2\pi(f_e - f_v)t - \beta_l + \frac{2\pi}{3}\right] \\ &\quad + i_{dr} \cos\left[2\pi(f_e + f_v)t - \beta_r + \frac{2\pi}{3}\right] \end{aligned} \tag{10}$$

where i_{dl}, i_{dr} are the lower sideband component at frequency $(f_e - f_v)$, and the upper sideband component at frequency $(f_e + f_v)$, respectively, two angles β_l and β_r denote the initial phase angle of the lower sideband and upper sideband components, respectively. With this assumption if $f_v < f_e$, it can be shown (in the same way as for a broken rotor bar) that Park's vector modulus will be equal to:

$$\begin{aligned} |i_d + j i_q|^2 &= \tfrac{2}{3}(i_f^2 + i_{dl}^2 + i_{dr}^2) + 3 i_f i_{dl} \cos(2\pi f_v t - \alpha + \beta_l) \\ &\quad + 3 i_f i_{dr} \cos(2\pi f_v t + \alpha - \beta_r) + 3 i_{dl} i_{dr} \cos(4\pi f_v t + \beta_l + \beta_r) \end{aligned} \tag{11}$$

Consequently, the Park's vector modulus spectrum is the sum of a dc level, generated mainly from the fundamental component of power supply, plus two additional terms at frequencies f_v and $2f_v$.

If $f_v > f_e$, it can be shown that Park's vector modulus will be equal to:

$$\begin{aligned} |i_d + j i_q|^2 &= \tfrac{2}{3}(i_f^2 + i_{dl}^2 + i_{dr}^2) + 3 i_f i_{dl} \cos(2\pi |2f_e - f_v| t - \alpha + \beta_l) \\ &\quad + 3 i_f i_{dr} \cos(2\pi f_v t + \alpha - \beta_r) + 3 i_{dl} i_{dr} \cos(4\pi f_e t + \beta_l + \beta_r) \end{aligned} \tag{12}$$

Consequently, the Park's vector modulus spectrum is the sum of a dc level, generated mainly from the fundamental component of the power supply, plus three additional terms at frequencies f_v, $2f_v$ and $|2f_v - f_e|$.

It can be seen that in both cases the fundamental power supply component is rejected completely. Another considerable point is that the amplitude of components related to the defect is multiplied by $3i_f$. Therefore, defects can be detected in incipient stages.

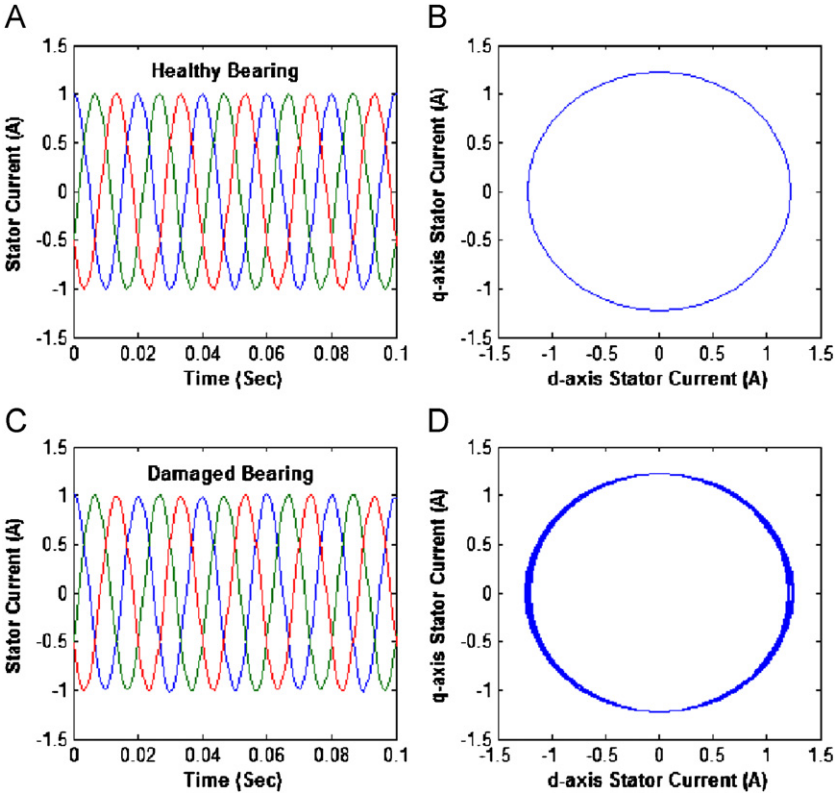

Fig. 2. Simulated stator current and *d–q* curves. (A) 3 phase current in healthy case, (B) d–q curve in healthy case, (C) 3 phase current in defective case and (D) d–q curve in defective case.

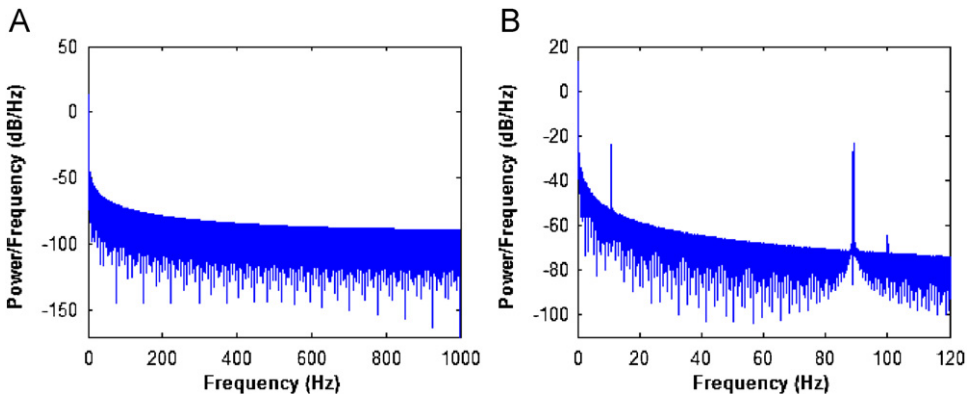

Fig. 3. Park's vector modulus spectrum. (A) Healthy case and (B) defective case.

5. Simulation results

In this section, an incipient fault is studied. In a healthy case, stator current is modeled by Eq. (9) with $f_e = 50$ Hz and $i_f = 1$ A, and for a defective case, it is modeled by Eq. (10) assuming $i_{dl} = i_{dr} = 0.01$ A and $f_v = 89$ Hz. In Fig. 2 simulated stator current and related d–q curves are illustrated. Comparing Fig. 2C and A shows that time-domain signals have not changed significantly. However, comparison of Fig. 2D with Fig. 2B shows clearly that thickness of Lissajou's curve is increased because of the harmonics generated by the defect. Therefore, using these curves is of great help for motor condition monitoring. Although faults can be detected by this method, it has a great drawback that requires a database for different practical situations. Hence, Park's vector modulus spectrum is proposed to solve this problem. These spectrums are illustrated in Fig. 3. As theoretically predicted, in both cases of motor condition (with and without defect), fundamental component of power supply is rejected completely. In a healthy case, only a dc component from the Park's current modulus spectrum exists, while in the defective case, characteristic defect component (89 Hz) and its side bands also exist. As it can be seen, the increase in the amplitude of the characteristic defect component proves the ability of this method compared to powerful methods such as wavelet transform [11].

6. Experimental result

The experimental setup consists of a 380 V, 1.2 kW, 50 Hz, 1400 rpm, three-phase, four-pole induction motor. Both shaft-end and fan-end bearings are 6205-2Z.

From the 6205-2Z bearing data sheet, the bearing dimensions are listed in Table 1.

Assuming equal thickness for the inner and outer races leads to a pitch diameter equal to 38.5 mm ($D = 38.5$ mm). Also assuming a contact angle (α) of 0°, and that the motor was operated at the measured shaft speed of 1498 rpm ($f_{rm} = 24.96$ Hz), the characteristic vibration frequencies are calculated from Eqs. (1)–(4), and the modulated frequency on stator current is derived by Eq. (5) as listed in Table 2.

Five tests were conducted to evaluate the ability of the proposed method. At first, while bearing was in a healthy condition (case A), the stored stator current was used as a baseline. In the second experiment, as shown in Fig. 4, a 1-mm hole was drilled on the outer race (case B), while in the third experiment a similar hole was drilled on the inner race (case C). Because inner race damage has more transfer segments when transmitting to the outer race surface of the case, usually the impulse components are rather weak in the vibration signals.

Table 1
Bearing dimensions

Parameter	Value
Outside diameter (mm)	52
Inside diameter (mm)	25
Ball diameter (mm)	7.938
Number of ball, n	9

Table 2
Characteristic vibration frequency and modulation effect on the stator current

Condition	Characteristic defect in vibration (Hz)	Modulation effect on stator current (Hz)
Defective outer race	89.2	39.2, 128.4, 139.2
Defective inner race	135.5	85.5, 185.5, 221
Distributed defect	117.5	66, 166, 182

Fig. 4. Defective bearing used in the second experiment.

Hence, diagnosis for inner race damages is very difficult [12]. Therefore, a 3-mm hole was drilled on the inner race to exaggerate the case (case D). At last, in order to study a distributed defect, two holes were drilled on the outer race (case E). In all tests, stator current was sampled at $F_s = 2$ kHz.

In the following, the proposed method is applied to the measured data. For this purpose, the d–q curves and Park's vector modulus spectrum of measured signals are computed and compared with the healthy status. First, d–q curves are drawn and fault effect is investigated in thickness and shape of Lissajou's curves.

Fig. 5 shows Lissajou's curve of the healthy motor. The curve is expected to have circular shape centered at origin. However, as it can be seen in Fig. 5, this curve is different from an ideal

condition. This apparent discrepancy between theory and observed machine data is due to two main reasons. First, virtually all voltage sources (three-phase or single-phase) contain some degree of asymmetry from one half-cycle to the next. Second, all electric machines contain some amount of inherent asymmetries. These asymmetries are both electrical (e.g., differences in stator winding impedances from phase-to-phase) and mechanical (e.g., the air gap is never perfectly symmetrical). Both types of asymmetries contribute to an impedance unbalance from phase-to-phase. Additionally, all three-phase voltage sources contain some difference in magnitude from phase-to-phase due to unequal loading of the phases (i.e., an unequal distribution of many single-phase loads on the three-phase source). The result from Fig. 5 is used as a baseline with respect to the case of the faulty motor. In Fig. 6, *d–q* curves related to the tests are shown (cases B–E). It is observed that the thicknesses of these curves are clearly increased compared to Fig. 5. As discussed earlier, this is because of the harmonics generated by the defect. Therefore, studying these curves can be used for fault detection. However, detection of fault location by this method alone is very difficult. Park's vector modulus spectrum is proposed to solve this problem. In Fig. 7A, Park's vector modulus spectrum of three-phase stator current for the healthy case is shown. It is expected ideally, that fundamental component and its harmonics be rejected completely. However, as discussed above, due to power supply asymmetry and also inherent asymmetries of motor, the fundamental component and its entire harmonics will be present in the stator current spectrum, and consequently in the Park's vector modulus spectrum (weakly), for all types of ac machines. The main point is to diminish the amplitude of the fundamental component, which does not need filtering. If the fundamental component is filtered, some information could be lost. Therefore, the presented method

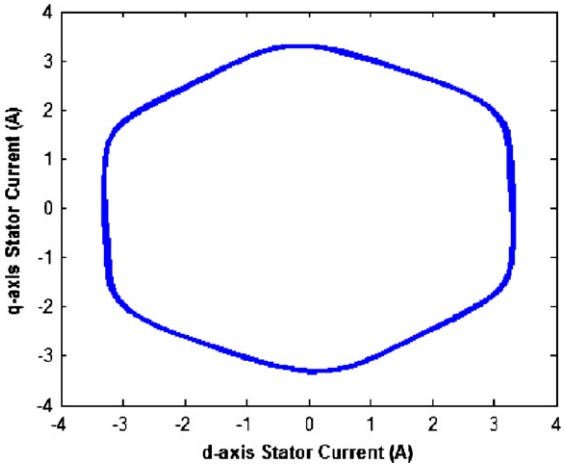

Fig. 5. Lissajou's curve of healthy condition.

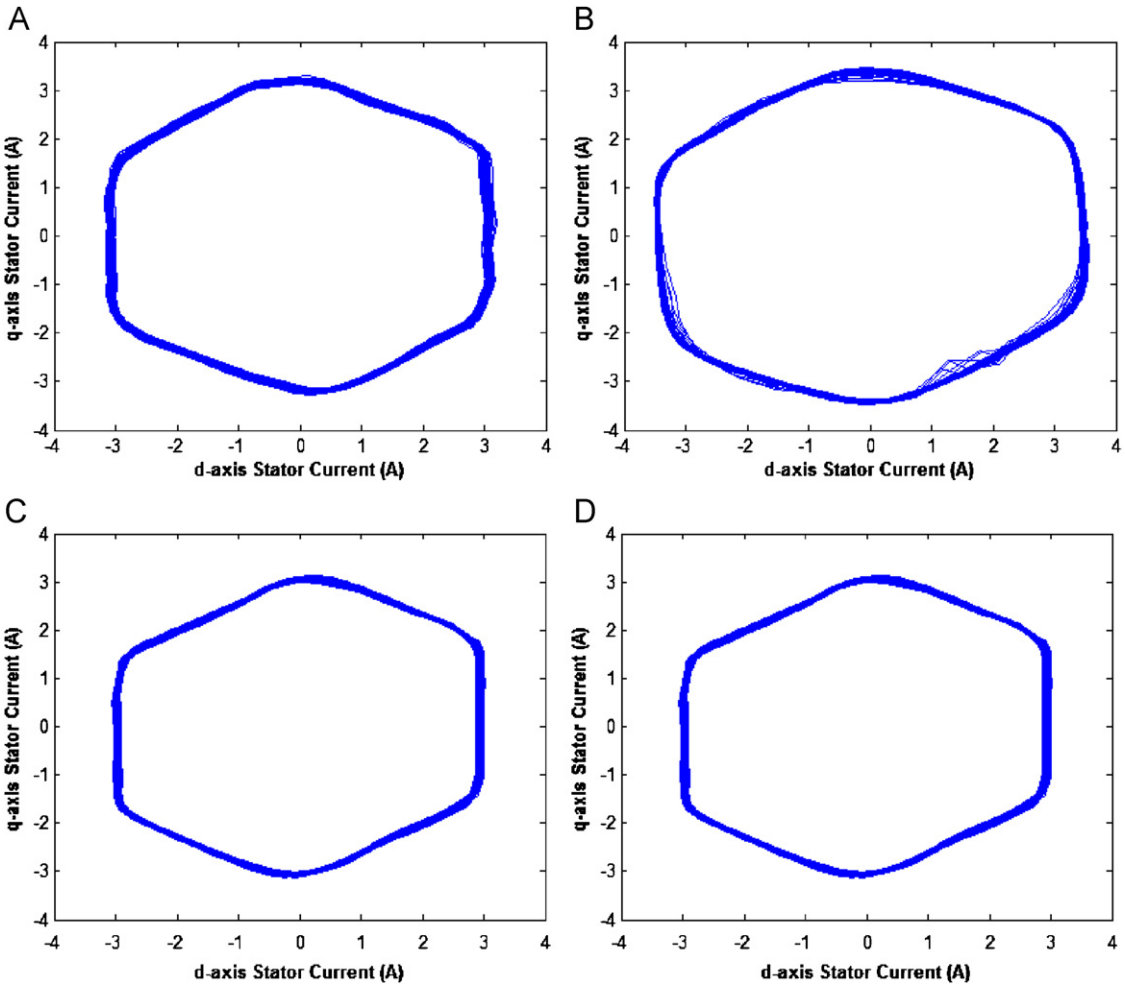

Fig. 6. Lissajou's shape of stator current Park's vector in various conditions. (A) Single 1-mm hole on the outer race, (B) single 1-mm hole on the inner race, (C) single 3-mm hole on the inner race and (D) double 1-mm hole on the outer race.

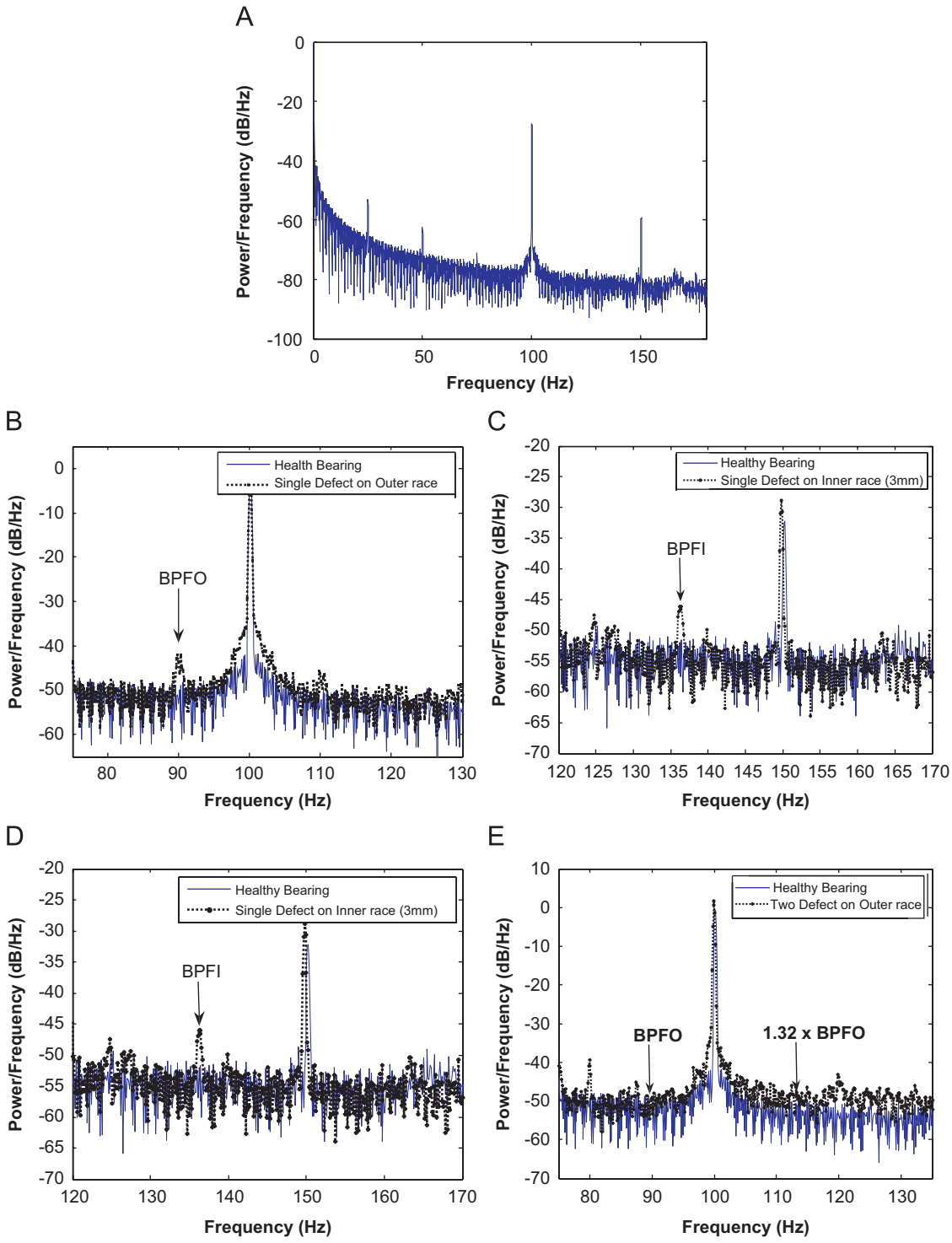

Fig. 7. Park's vector modulus spectrum in defective cases. (A) Park's vector modulus spectrum in healthy case, (B) case of single 1-mm hole on the outer race (case B), (C) case of single 1-mm hole on the inner race (case C), (D) case of single 3-mm hole on the inner race (case D) and (E) case of double 1-mm hole on the inner race (case E).

keeps all information that provides better fault detection. Besides, it should be noted that the characteristic defect frequency is the same in Park's vector modulus and vibration signal. This fact can easily be verified as well from Eqs. (11) and (12).

In the following, Park's vector modulus spectrums of the experiments are investigated. In case B, corresponding to a local defect in the outer race, a 89.2 Hz component is produced in vibration signals. It is expected that same component be generated in Park's vector modulus spectrum. A segment of Park's vector modulus spectrum around 89 Hz is shown in Fig. 7B. Amplitude in the faulty case (dot line) is obviously increased in 89.2 Hz compared to the healthy case (continuous line). Park's vector modulus spectrum for case C where a 1-mm hole was drilled on the inner race is shown in Fig. 7C. It can be seen that the amplitude of related signal to faulty case is increased in 135.5 Hz which shows the superiority of this method. By increasing fault severity (case D), related component to fault is increased which is shown in Fig. 7D.

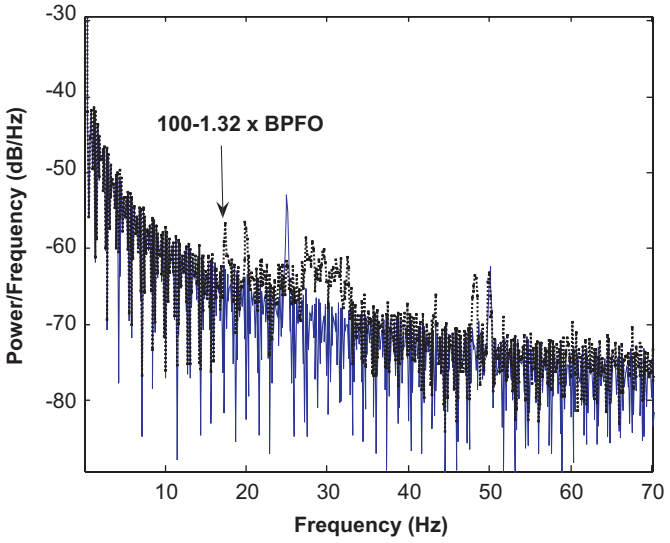

Fig. 8. Park's vector modulus spectrum of case D around 17 Hz.

In the pervious experiments local defects was studied. In the following, distributed defect is investigated. For this purpose, two 1-mm holes were drilled on the outer race (case E). Zoomed Park's vector modulus spectrum of the case is shown in Fig. 7E. As can be seen, no component is produced in 89.2 Hz. Vibration signals for this case were studied in Ref. [17]. The results from vibration signals analysis also show that no component is produced in 89.2 Hz, and instead, a 117 Hz component is generated. Based on Eq. (12) components produced by the defect are 17, 117, 184, … Hz. Amplitude of faulty signal is increased slightly in these frequencies. Park's vector modulus spectrum around 17 Hz is shown in Fig. 8; the rise in amplitude in 17 Hz is clear. This case shows that relations (1)–(4) are usable in the case of a local defect only. Otherwise, the generated component is a multiplication of the characteristic defect frequency.

Another considerable point is that the characteristic ball defect frequency is 116 Hz, and if the case was not predetermined, it could be miss-detected.

7. Conclusions

Conventional methods of bearing damage detection like other mechanical apparatus are based on vibration analysis. As, current transducers are cheaper than vibration transducers and MCSA can also detect the bearing defects successfully, an advanced current signal processing can be a suitable alternative for fault detection. In this study, an approach based on Park's vector for the monitoring of induction motors by computer is used as a simple diagnostic method for the detection of incipient bearing failures via stator current analysis. Bearings fault detection can be easily obtained by observing the thickness of the Lissajou's curves. However, in this method many data from different cases should be gathered and hence a comprehensive database is needed to classify faults. In order to solve this problem, an approach based on spectral analysis of the motor current Park's vector modulus is used.

In this approach increase of characteristic component amplitude is a linear function of the severity of fault. Simulation and experimental results from a three-phase induction motor shows the superiority of the proposed method compared to the conventional methods.

References

[1] Benbouzid MEH. Bibliography on induction motors faults detection and diagnosis. IEEE Trans Energy Convers 1999;14(4):1065–74.
[2] Thomson WT. A review of on-line condition monitoring techniques for three-phase squirrel cage induction motors—past present and future. In: IEEE SDEMPED'99, Spain, September 1999. p. 3–18.
[3] Singh GK, AlKazzaz SAS. Induction machine drive condition monitoring and diagnostic research—a survey. J Electr Power Res 2003;64:145–58.
[4] Nandi S, Toliat HA, Li X. Condition monitoring and fault diagnosis of electrical motors—a review. In: IEEE industry applications conference, thirty-fourth IAS annual meeting, vol. 1, 1999. p. 197–204.
[5] Schoen RR, Habetler TG, Kamran F, Bartheld RG. Motor bearing damage detection using stator current monitoring. IEEE Trans Ind Appl 1995;32(6):1274–9.
[6] Benbouzid MEH. A review of induction motors signature analysis as a medium for faults detection. IEEE Trans Ind Electron 2000;47(5):984–93.
[7] Benbouzid MEH. What stator current processing-based technique to use for induction motor rotor faults diagnosis? IEEE Trans Energy Convers 2003;18(2):238–44.
[8] Tandon N, Choudhury A. A review of vibration and acoustic measurement methods for the detection of defects in rolling element bearings. J Tribol Int 1999;32(8):469–80.
[9] Yazici B, et al. An adaptive, on-line, statistical method for bearing fault detection using stator current. In: IEEE annual meeting, New Orleans, Lousiana, 5–9 October 1997.
[10] Yazici B, Kliman GB. An adaptive statistical time–frequency method for detection of broken bars and bearing faults in motors. Issue Series Title: IEEE Trans Ind Appl 1999;35(2).
[11] Zarei J, Poshtan J. Bearing fault detection using wavelet packet transform of induction motor stator current. J Tribol Int 2007;40(5):763–9.
[12] Prabhakar S, Mohanty AR, Sekhar AS. Application of discrete wavelet transform for detection of ball bearing race faults. J Tribol Int 2002;35(12):793–800.
[13] Nikolaou NG, Antoniadis IA. Rolling element bearing fault diagnosis using wavelet packets. J NDT&E 2002;35(3):197–205.
[14] Haji M, Toliyat HA. Pattern recognition—a technique for induction machines rotor broken bar detection. IEEE Trans Energy Convers 2001;16(4):312–7.
[15] Benouzza N, Benyettou A, Bendiabdellah A. An advanced Park's vectors approach for rotor cage diagnosis. In: Proceeding of first international symposium on control, communications and signal processing, 2004. p. 461–4.
[16] Eltabach M, Charara A, Zein I. A comparison of external and internal methods of signal spectral analysis for broken rotor bars detection in induction motors. IEEE Trans Ind Electron 2004;51(1):107–21.
[17] Zarei J. Induction motor bearings fault detection using stator current analysis compared to vibration analysis. MSc thesis, Iran University of Science and Technology, Iran, March 2005 [in Persian language].
[18] Zarei J, Poshtan J. A new method based on Park's vectors approach for bearing fault detection. In: Proceeding of 20th international power system conference, Tehran (Iran), 16–18 November 2005 [in Persian language].
[19] Zarei J, Poshtan J. An advanced Park's vectors approach for bearing fault detection. In: Proceedings of the IEEE international conference on industrial technology (ICIT), India, 15–17 December 2006. p. 1472–9.
[20] Silva JLH, Marques Cardoso AJ. Bearing failures diagnosis in three-phase induction motors by extended Park's vector approach. In: Proceedings of the IEEE IECON'05, Raleigh, NC, USA, November 2005. p. 2591–6.